HOKKAIDO UNIVERSITY

Title	Genetic analysis of phenotypes caused by deficiency in the development of neural crest-derived cells in the rat
Author(s)	王, 金曦; Wang, Jinxi
Degree Grantor	北海道大学
Degree Name	博士(獣医学)
Dissertation Number	甲第13726号
Issue Date	2019-09-25
DOI	https://doi.org/10.14943/doctoral.k13726
Doc URL	https://hdl.handle.net/2115/90300
Type	doctoral thesis
File Information	Jinxi_WANG.pdf

Genetic analysis of phenotypes caused by deficiency in the development of neural crest-derived cells in the rat

（ラットにおける神経堤細胞由来細胞の発達の欠陥によりもたらされる表現型の遺伝学的解析）

Jinxi Wang

Laboratory of Laboratory Animal Science and Medicine

Department of Applied Veterinary Science

Graduate School of Veterinary Medicine

Hokkaido University

Japan

Abbreviations

AChE	Acetylcholinesterase
AGH	Aganglionosis Hokkaido rat
bp	Base pair
Chr	Chromosome
CI	Confidence interval
cM	Centi-morgan
Ednrb	Endothelin receptor type B gene
EMT	Epithelial-to-mesenchymal transition
ENCCs	Enteric neural crest cells
ENS	Enteric nervous system
ERV	Endogenous retrovirus
h	hour
HSCR	Hirschsprung disease
LRS	Likelihood ratio statistic
LTR	Long terminal repeat
Min	Minutes
NC	Neural crest

NCCs	Neural crest cells
PCR	Polymerase chain reaction
PNS	Peripheral nervous system
QTL	quantitative trait locus
RGD	Rat Genome Database
sec	seconds
sgRNA	single guide RNA
sl	spotting lethal
SNP	single nucleotide polymorphism

Table of Contents

LIST OF TABLES

LIST OF FIGURES

Preface

The neural crest (NC) is one of the most pluripotent embryonic tissues in vertebrates and is considered as "explorers of the embryos" due to its extensive ability of migration and differentiation. The neural crest cells (NCCs) are specified at the border of the neural plate after gastrulation. During neurulation, the borders of neural plate become thick and converge at the midline of dorsal, forming the neural tube. After a process of epithelial-to-mesenchymal transition (EMT), the NCCs are separated from the neuroepithelium, depart from the roof plate of the neural tube and start migration (1). These stem-like cells migrate throughout the embryo to colonize a myriad of tissues and organs including the cartilage and bone of the head, nerve ganglia, smooth muscle, connective tissue, heart, enteric ganglia, peripheral nervous system (PNS), secretory cells of the endocrine system and pigment cells of the skin (2). The development of these tissues including the processes of migration, proliferation and differentiation of the NCCs is regulated by multiple genes and signaling pathways (3, 4). Mutations of these genes always cause abnormal development of the related NC-induced tissues or organs and lead to various congenital disorders, such as frontonasal dysplasia, Waardenburg-Shah syndrome and DiGeorge syndrome (5-7). According to the current reports, more than 700 different syndromes are related to aberrant neural crest

developmental (8). The involved regulatory gene networks have been widely studied, especially in the last several decades; however, there are still vast genetic mechanisms unrevealed.

In this study, two disorders caused by the abnormal development of two different NCCs-derived cell linages were investigated in laboratory rats and it was found that the symptoms or phenotypes of these disorders were significantly modified by the genetic background.

The first disorder is aganglionosis caused by agenesis of enteric nervous system (ENS). ENS is the most complex division of the PNS, principally originates from vagal NC and partly originates from sacral NC (9). During the mice embryogenesis, the migrating vagal NCCs invade the foregut at E9 - E9.5 and are referred to as enteric neural crest cells (ENCCs). In the following 5 days, these ENS progenitor cells colonize along the developing gut, proliferate and differentiate into neurons and glia (9, 10). In the same period, sacral NCCs also migrate ventrally to form extrinsic pelvic ganglia, later enter hindgut when the vagal NCCs reach the terminal of intestinal canal (11, 12). This colonization of ENCCs is regulated by multiple genes that are involved in different signaling pathways. Mutations of the related genes can easily stop this process and lead to aganglionosis in the residual segments of the canal. Endothelin receptor type B gene

(*Ednrb*) is one of the genes that play critical roles in regulating ENCCs development. In Chapter 1, the generation of a new *Ednrb* mutated rat strain was tried and it has been found that the combination of *Ednrb* null mutation with a certain genetic background causes the embryonic death, which provides new clues for the investigations of gene-regulatory network related to the development of ENS and embryogenesis.

The second disorder investigated in this study is the hooded phenotype in laboratory rats, which is caused by the incomplete distribution of melanocyte in the skin. The melanocytes are derived from trunk NCCs. During the embryonic development, the unpigmented melanocytic progenitors, melanoblasts, are differentiated from trunk segment of neural crest and migrate into the developing follicles and give rise to the melanocytes, which can synthesize melanin (13). The development of melanocytes is also regulated by multiple genes, such as paired box 3 gene (*Pax3*), microphthalmia-associated transcription factor gene (*Mitf*), sex-determining region Y-box 10 (*Sox10*), c-Kit tyrosine kinase receptor gene (*Kit*), endothelin 3 gene (*Edn3*), *Ednrb*, etc. (14). Among these, the *Kit* gene plays a critical role in migration, differentiation, proliferation, and survival of melanocytic system. Hooded mutations occur in the first intron of *Kit* gene and lead to various extents of pigmentation deficiency (15). In Chapter 2, quantitative trait locus (QTL) analysis was conducted

using two rat strains, which carried the same mutation on the *Kit* gene, referred as hooded, but showed different extents of hair pigmentation. By means of this analysis, a QTL responsible for modifying hooded phenotype was detected on chromosome (Chr) 17. This result proceeds the identification of a new gene that regulates melanocyte development.

Chapter 1

Null mutation of the endothelin receptor type B gene causes embryonic death in the GK rat

1.1. Introduction

The ENS is an important and complex part of the visceral nervous system in vertebrates, originates from NC cells and extends into the wall of the alimentary canal along the entire length of that canal (9). Under the regulation of the ENS, the intestine is capable of motility, including contraction and relaxation, which causes the intestinal tract contents to be passed along and feces to be expelled from the anus. Hirschsprung disease (HSCR) is a common congenital disorder of the gastrointestinal tract that occurs in about 1/5000 live births (16). It is characterized by a defective ENS caused by the incomplete migration, differentiation, and proliferation of NC cells in the gastrointestinal track in the early embryonic stage (17). The affected portion of the intestines is always a continuous portion of the caudal gastrointestinal tract and obstructs the smooth passage of stool (18). Patients with this disease suffer from constipation of varying severity, including complete obstruction, depending on the length of the aganglionic section (16, 19, 20).

In HSCR, the penetrance and phenotypes of aganglionosis segment length vary by gender and familial incidence. The variation in phenotypes is attributed to the complex genetic interactions between discovered and unrevealed susceptibility loci or modifier loci in different genetic backgrounds, which regulate the development of ENS (17, 19).

A series of genetic studies have already implicated several genes, including the *RET* proto-oncogene (21), the *EDNRB* (22-24), the *EDN3* (25), the glial-cell-line-derived neurotrophic factor gene (*GDNF*) (26, 27), the *SOX10* (7), the neurturin gene (*NRTN*) (28), the endothelin converting enzyme 1 gene (*ECE1*) (29), the zinc finger homeobox 1B gene (*ZFHX1B*) (30), the paired-like homeobox 2B gene (*PHOX2B*) (31), the KIF1 binding protein gene (*KIF1BP*) (32), and the transcription factor 4 gene (*TCF4*) (29). Of these, the *EDNRB* gene, which is involved in the EDN3/EDNRB signaling, is known to play a key role in the development of HSCR, as either the heterozygous or homozygous mutation of this gene is found in HSCR patients (23, 33, 34).

The spotting lethal (*sl*) mutation occurs naturally as a null mutation in the rat *Ednrb*, which displays a 301-bp deletion that leads to dysfunction of the corresponding protein (35). In previous studies, three inbred and congenic rat strains carrying the *sl* mutation on *Ednrb* were produced, and named as AGH (aganglionosis Hokkaido)-*Ednrb*[sl], LEH (Long-Evans Hokkaido)-*Ednrb*[sl], and F344-*Ednrb*[sl] (36). The symptoms caused by this mutation differ according to the genetic background. The AGH-*Ednrb*[sl] displayed the most severe symptom of megacolon with a very low survival rate until weaning. The ratio of aganglionic length to large intestine length of this strain was more than 2.0. On the other hand, the LEH-*Ednrb*[sl] and F344-*Ednrb*[sl] displayed much milder symptom,

and most of the F344-*Ednrb^{sl}* can survive with a small aganglionic region. The ratios of

aganglionic length to large intestine length of the LEH-*Ednrb^{sl}* and F344-*Ednrb^{sl}* were

0.5 and less than 0.5, respectively. (36). The QTL analysis on the AGH-*Ednrb^{sl}* and the

LEH-*Ednrb^{sl}* or F344-*Ednrb^{sl}* rats, using the ratio of aganglonic intestine length to large

intestine length as the quantitative trait, identified a QTL on Chr 2 as being responsible

for this variation (37, 38). Comparisons of the sequence of genes located in the

identified region of these three rat strains revealed different haplotypes between the rats

that presented severe symptoms and those that presented mild symptoms (38),

suggesting that different haplotypes of this region caused the variation in the symptoms

of HSCR resulting from the *Ednrb^{sl}* mutation. However, the AGH-*Ednrb^{sl}*, which

displayed the most severe symptoms, went extinct for unknown reason. To continue the

study of phenotypes of the *Ednrb^{sl}* mutation by creating a new rat model with the

Ednrb^{sl} mutation that shows severe symptoms, the GK/Slc inbred rat strain was selected

from database, as the haplotype of the responsible region is similar to that of the AGH

rat. In this study, by preparing F$_2$(GK × F344)-*Ednrb^{sl/sl}* progeny and genome-edited GK

rats, it has been found that the null mutation of the *Ednrb* gene causes the more serious

symptoms of early embryonic death in GK rats, suggesting that the haplotype of Chr 2

plays an important role in regulating the phenotype of HSCR caused by the *Ednrb*

mutation.

1.1 Materials and Methods

1.1.1. Animals

F344, GK, and SD rats were purchased from Japan SLC, Inc. (Hamamatsu,

Shizuoka, Japan). The F344-*Ednrb$^{sl/+}$* rats were obtained as described previously (36).

Male F344-*Ednrb$^{sl/+}$* rats were mated with female GK rats to produce the F_1 generation,

and the F_2 progeny were generated by mating the heterozygous F_1 offspring. The

animals were maintained in specific pathogen-free conditions with feeding and drinking

allowed *ad libitum*. All rats including 10-day-old F_2 progeny and pregnant females were

euthanized by inhalation of CO_2 following the AVMA Guidelines for the Euthanasia of

Animals: 2013 Edition. Fetuses collected from euthanized pregnant females were

euthanized by decapitation. All research and experimental protocols were conducted

according to the Regulation for the Care and Use of Laboratory Animals of Hokkaido

University and Osaka University, and were approved by the Animal Care and Use

Committees of Hokkaido University (Approval ID: No. 14-0155 and 15-0111) and

Osaka University (Approval ID: 動医 28-060-037, this approval is based on the

permission for the gene manipulation (（遺）4160).

1.1.2. Genotyping *Ednrb* and microsatellites

The *Ednrb* genotype was identified by primer set 1 (F-CCTCCTGGACTAGAGGTTCC and R-ACGACTTAGAAAGCTACACT). DNA samples were obtained from the tail tips or tissue by using a KAPA Express Extract DNA Extraction Kit (Kapa Biosystems, London, UK). PCR products were electrophoresed in 1.5% agarose gels to distinguish the wild alleles (517 bp) from the mutant alleles (216 bp). The microsatellite markers *D2Rat174*, *D2Rat201*, *D2Rat19*, and *D2Mgh21* were selected for identification of the haplotype of each F_2 progeny in the responsible region, according to their location relative to the *Gdnf*, *Ptger4*, and *Slc45a2* on Chr 2 in the Rat Genome Database (RGD, https://rgd.mcw.edu). The positions of the genes and microsatellite markers were based on information from the RGD (assembly Rnor_6.0) (https://rgd.mcw.edu/wg/). All PCR products were electrophoresed in 10% polyacrylamide gels, stained with ethidium bromide, and photographed under an ultraviolet lamp.

1.1.3. Knockout of *Ednrb* and *Rosa26* by CRISPR/Cas9

The single guide RNA (sgRNA) for *Ednrb* was designed to target the sequence 5'-AGCCGGTGCGGACGCGCCTTGG-3' on exon 2 of *Ednrb*. sgRNA for *Rosa26* was designed to target the sequence 5'- GACTCCAGTTGCAGATCACG -3' on exon 1 of

Rosa26. sgRNAs were transcribed *in vitro* using a MEGAshortscript T7 Transcription Kit (Thermo Fisher Scientific, Carlsbad, CA, USA) from synthetic double-stranded DNAs obtained from Integrated DNA Technologies, IA, USA or Thermo Fisher Scientific. The pCas9-poly was formally constructed and deposited into the Addgene repository (ID #72602; www.addgene.org/CRISPR). mRNA was transcribed *in vitro* using a mMESSAGE mMACHINE T7 Ultra Kit (Thermo Fisher Scientific) from linearized plasmids and was purified using a MEGAClear kit (Thermo Fisher Scientific).

Super ovulation was induced in female GK and F344 rats by injecting with 150 U/kg pregnant mare serum gonadotropin and 48h later 75 U/kg human chorionic gonadotropin. The super-ovulating female rats were mated with male rats of the same strain. The female rats confirmed to have copulatory plugs were euthanized by the inhalation of CO_2 and the following morning pronuclear-stage embryos were collected. The sgRNA for *Ednrb* and *Rosa26* and Cas9 mRNA were introduced into embryos using a NEPA21 Super Electroporator (Nepa Gene, Ichikawa, Japan). The embryos that developed into 2-cell embryos were collected and transferred into the oviducts of female surrogate SD rats anesthetized with isoflurane.

1.1.4. CRISPR-mediated mutation analysis

DNA samples from the puerperal offspring of the GK and F344 strains were prepared from tail tips. Primer set 2 (F-GGCGCGCAAACTTAACTTAC and R-GGGACCATTTCTCATGCACT) flanking a 583-bp sequence, including the targeting sequence of sgRNA on *Ednrb*, and primer set 3 (F- TGCTCTCCAAAAGTCGGTTT and R-CCCAGGTGAGTGCCTAGTCT) flanking a 391-bp sequence, including the targeting sequence of sgRNA on *Rosa26*, were designed to amplify the targeting sequence. PCR was performed in a total volume of 15 µl under the following conditions: 1 cycle at 94°C for 3 min; 35 cycles of 94°C for 30 s, 60°C for 1 min, and 72°C for 45 s; and 1 cycle at 72°C for 3 min. The PCR products were then directly sequenced using a BigDye Terminator v3.1 Cycle Sequencing Kit and the standard protocol for an Applied Biosystems 3130 DNA Sequencer (Thermo Fisher Scientific).

1.1.5. Acetylcholinesterase (AChE) staining

The whole intestine (from pylorus to anus) was dissected from the 10-day-old pups of F_2(GK × F344) and genome-edited F344 rats. After the attachments and contents were removed, the intestine was subjected to AChE whole-mount staining (39). Visualization of the enteric ganglia and measurement of the aganglionic length were conducted under a microscope. The ratio of the affected length to the length of the large

intestine was calculated to determine the severity of aganglionosis as described

previously (36).

1.2. Results

1.2.1. Selection of a rat strain possessing a similar haplotype in the responsible region of Chr 2 in order to create a new rat model that shows the severe symptoms of aganglionosis.

Previous studies identified a QTL on Chr 2 as responsible for controlling the severity of aganglionosis in the rat model carrying the *Ednrb* null mutation (37, 38). It has been indicated that several SNPs on three genes, *Gdnf*, *Slc45a2*, and *Ptger4*, located in this region constitute different haplotypes between the rat strains showing mild versus severe symptoms (38). To verify whether the haplotype of these SNPs modifies the symptoms caused by *Ednrb* mutations and to create a new rat model that displays the severe symptoms, the sequence polymorphisms of the recorded rat strains in the RGD were investigated to identify any rat strains possessing a haplotype similar to that of the AGH rat. According to the information in the database, the GK rat strain was found to display the most similar haplotype to that of the AGH rat among registered inbred strains. The haplotype of the GK/Slc rat (Table 1) was determined using the method described in a previous paper (38). The positions of the genes and microsatellite markers are based on information from Rattus norvegicus (assembly Rnor_5.0).

1.2.2. F_2(GK × F344)-$Ednrb^{sl}$ progeny with the GK haplotype in the responsible region on Chr 2 experience embryonic death

To verify that the haplotype of responsible region in the GK rat also causes the severe symptoms that are seen with the mutant $Ednrb$, F_2(GK × F344) progeny were produced by mating GK females to F344-$Ednrb^{sl/+}$ males and crossing the heterozygous F_1 progeny. Fifty 10-day-old F_2(GK × F344) progeny were harvested. After genotyping and histological analysis, it was found that F_2(GK × F344)-$Ednrb^{sl/sl}$ progeny presented various extent of aganglionosis, including the severe symptoms similar to those seen in the AGH-$Ednrb^{sl/sl}$ rat (Fig. 1A, 1B), suggesting that the genetic background of the GK inbred strain exacerbates the extent of aganglionosis severe. To easily determine the haplotype of the responsible region in the F_2 progeny, 4 microsatellite markers ($D2Rat201$, $D2Rat174$, $D2Rat19$, and $D2Mgh21$) located in the responsible region including the three candidate genes were selected (Fig. 1C). After performing genotyping, it was found that two progeny, progeny 1 and progeny 2, which showed the severe symptoms of aganglionosis possessed heterozygous haplotype in the responsible region, suggesting that the GK rat may carry the modifier gene(s) responsible for the severity of aganglionosis in the responsible region. Other F_2 progeny showing much milder symptoms of aganglionosis possessed either the heterozygous or the

F344-homozygous haplotype (Fig 1B). Notably, no GK-homozygous F_2 progeny were

obtained (Fig 1B). Therefore, it was hypothesized that the progeny carrying the

GK-homozygous haplotype in the responsible region displayed more severe symptoms

that caused them to die in the prenatal stages if they carried the *Ednrb* mutation. To test

this hypothesis, the number of F_2 progeny was compared for each haplotype of the

responsible region in all 50 F_2 progeny, including the wildtype rats, the heterozygous

Ednrb^{sl} rats, and the homozygous *Ednrb^{sl}* rats (Table 2). In 43 healthy F_2 progeny

possessing either the wildtype or the heterozygous *Ednrb^{sl}* mutation, the numbers of

F344-homozygous, heterozygous, and GK-homozygous genotypes of each

microsatellite followed an approximately 1:2:1 ratio, in agreement with the Mendelian

rule. However, F_2 progeny possessing the GK-homozygous genotype were not obtained

in the homozygous *Ednrb^{sl}* mutation. Further, 29 embryos of the F_2(GK × F344)

generation were investigated at the E16 stage. The results were consistent with those for

10-day-old offspring, i.e., no F_2(GK × F344)-*Ednrb^{sl/sl}* embryos carried the GK

haplotype (data not shown). These data strongly suggest that the combination of the

homozygous *Ednrb^{sl}* mutation and the GK haplotype in the responsible region on Chr 2

are what cause embryonic death.

1.2.3. Targeted disruption of *Ednrb* by genome editing in GK rats.

The absence of F_2(GK × F344)-*Ednrb*$^{sl/sl}$ progeny carrying the GK haplotype in the

responsible region led investigation to examine whether the disruption of the *Ednrb* can

cause embryonic death in the GK inbred strain and can cause the related embryonic

phenotype. To verify this hypothesis, the CRISPR/Cas9 system was employed to

knockout the *Ednrb* in the GK strain. The genome editing experiments were also

performed in the F344 rat as a control. The sgRNA was designed targeting on exon 2 of

Ednrb in the rat. The technique for animal knockout system by electroporation (TAKE)

method was used to produce the genome-edited rat (40). After introducing the Cas9

mRNA and sgRNA-*Ednrb* into the zygotes collected from the F344 strain by

electroporation, twenty-three 2-cell embryos were transferred into the oviducts of one

surrogate rat, and 4 pups were obtained (Table 3). After the targeted sequence of these

four offspring were analyzed, two of the offspring were identified as bi-allelic knockout,

one carried a 14-bp deletion and a 16-bp deletion, and another carried a 2-bp deletion

and a 13-bp deletion in the two alleles. These deletions all caused the frame shift. The

other two littermates were found to carry the wildtype allele. The intestines of these

offspring were collected at postnatal day 10 and subjected to whole-mount AChE

staining. The two offspring carrying the deleted alleles were confirmed to show

aganglionosis in a small proportion of the large intestine (0.14 and 0.18). The results

from the F344 rats verified the efficiency of the TAKE method and the sgRNA. Then,

zygotes collected from the GK rat were transfected with Cas9 mRNA and

sgRNA-*Ednrb* using the same method and eighty-eight 2-cell embryos were transferred

into the oviducts of 4 surrogate female rats. However, only one female rat gave birth, to

2 pups which died soon after birth, and were eaten by the surrogate mother. Only a part

of one tail was left. Examination of the targeted sequence of genome DNA extracted

from the tail clip identified two kinds of alleles. One allele was the wildtype, and the

other carried a 35-bp deletion. After dissecting the uterus of the surrogate rats, tiny

implantation sites were found, indicating that most of the embryos had died after

implantation. These results suggest that the disruption of *Ednrb* caused embryonic death.

Genome editing on an unrelated gene, *Rosa26*, was performed in the GK rat using the

same procedure and conditions to test the above hypothesis. It was found that only 2.8%

of the transferred embryos survived to birth, and both of these were

heterozygote/mosaic (Table 3). The low reproduction rate of the *Rosa26*-modified GK

rats suggests that the genome editing procedure itself causes embryonic death in the GK

rat, indicating that it is impossible to use the genome editing strategy to verify that

Ednrb knockout causes the embryonic death in the GK rat.

1.3. Discussion

Ednrb, a critical gene in the development of HSCR, encodes a G-protein-coupled receptor for the ligand of EDN3 and is expressed primarily by migrating ENCCs (9). Generally, mutations of this gene cause pigmentary abnormalities, deafness and aganglionosis in humans and many other higher organisms (19, 41). These common phenotypes were also observed in the previous rat models, which carry a spontaneous null mutation in *Ednrb* (36). This null mutation caused severe aganglionosis in one of these rat strains, the AGH strain, leading to a lethality during the weaning stage, which is distinct from the other rat models. In this study, it was also found that the *Ednrb* mutation caused much greater lethality in the embryonic stage in the GK inbred rat strain. A similar phenotype was found in studies of the *Ednrb*$^{s-1Acrg}$ mutation, a 1.3-cM deletion on Chr 14, flanking the *Ednrb* gene in the mouse genome (42). This deletion also causes embryonic death in the early gestational period, and the homozygous embryos displayed gross morphological defects including poorly developed head folds and caudal truncation. The number of homozygous embryos was distinctly decreased at E11.5, and there were no homozygous embryos after E12.5 during embryogenesis. Similarly, another *Ednrb*$^{s-36Pub}$ mutation, which partly overlaps the *Ednrb*$^{s-1Acrg}$ deletion, leads the death of homozygous offspring at birth, which are consistent with the

phenotype of the *Ednrb^s-1Acrg* heterozygous mice (43). Studies of the genes and loci on this large deletion have proved the embryonic lethality in this case to require the loss of multiple genes and to involve complicated genetic mechanisms that remain unclear (43).

In this study, it was also found that the embryonic death was caused by the mutation of the *Ednrb* gene in the GK inbred strain. As the GK rat was confirmed to carry a haplotype in the responsible region on Chr 2 similar to that of the AGH rat presenting severe aganglionosis, it was expected that the *Ednrb*-null mutation to lead to the similar severe symptoms in the GK inbred strain. But even though some of the F_2(GK × F344)-*Ednrb^sl/sl* progeny displayed severe aganglionosis, no mutant progeny with the GK-homozygous haplotype in the responsible region were reproduced. To verify the embryonic death of the *Ednrb*-mutant GK rats, genome editing was conducted to generate *Ednrb*-null GK rats. Editing of the *Ednrb* gene caused the production of fewer offspring than for the control rat, F344. However, the genome editing of an unrelated gene, *Rosa26*, in GK rats with the same methods caused the production of similarly few offspring, suggesting that the genome editing itself caused the embryonic death in the GK rat. It is unknown at present what procedure in the genome editing causes the embryonic death in the GK rat.

The GK strain is a classical rat model of non-insulin-dependent diabetes mellitus

(NIDDM) (44). These animals always present symptom of type 2 diabetes, such as fasting hyperglycemia, impaired insulin secretion in response to glucose, and insulin resistance; however, these symptoms all appear at the young adult stage of 8 weeks old in the GK/Slc inbred strain (45), suggesting that the diabetes is not related to the embryonic death. Several studies have already identified a series of genetic loci that relate to the diabetes phenotype of the GK inbred strain (44, 46, 47). These loci are located on multiple chromosomes, but none of them overlaps the responsible region for the modifier of the aganglionosis phenotype on Chr 2. These data add evidence that the embryonic lethal phenotype is independent of the diabetes symptoms in the GK inbred strain.

The responsible region on Chr 2 includes another critical gene, *Gdnf*, which relates to the survival, proliferation, migration, and differentiation of ENCCs (38, 48). Some studies have found that patients with HSCR carry heterozygous mutation on the *Gdnf* and that *Gdnf*$^{/+}$ mice also show an approximately 50% reduction in ENCC number (26, 49). A *vitro* studies also elucidated that the combination of the AGH-type SNPs in the *Gdnf* promoter reduces *Gdnf* expression (50). Other studies have revealed that *Gdnf*$^{/-}$ animals always die within 24 h after birth and that after the first 24 h, the *Gdnf*$^{/+}$ animals died, too (51-53). Thus, considering the role of *Gdnf* in the development

of ENS, it is speculated that *Gdnf* plays a critical role in modifying the symptoms caused by the *Ednrb* mutation in the rat models used in this study. However, the AGH-*Ednrb^{sl}* rats, whose haplotype in the responsible region on Chr 2 is mostly consistent with that of the GK strain, were able to survive until 3 weeks old, whereas GK rats with a mutation of *Ednrb* showed embryonic death, suggesting that some other modifiers relating to the early embryonic death may exist in the genetic background of the GK rat. It is suggested that the GK rat can be valuable as a laboratory animal model for studying the interaction of genes involved in HSCR disease and embryogenesis. Further studies that uncover the modifier genes and genetic mechanisms in the GK rat strain promise to facilitate the understanding of the regulatory network of genes for the embryogenesis and development of ENS and HSCR.

1.4. Summary

The HSCR is an inherited disease that is controlled by multiple genes and has a complicated genetic mechanism. HSCR patients suffer from various extents of constipation due to dysplasia of the ENS, which can be so severe as to cause complete intestinal obstruction. Many genes have been identified as playing causative roles in ENS dysplasia and HSCR, among them the *Ednrb* has been identified to play an important role. Mutation of *Ednrb* causes a series of symptoms that include deafness, pigmentary abnormalities, and aganglionosis. In the previous studies of three rat models carrying the same *sl* mutation on *Ednrb*, the haplotype of a region on Chr 2 was found to be responsible for the differing severities of the HSCR-like symptoms. To confirm that the haplotype of the responsible region on Chr 2 modifies the severity of aganglionosis caused by *Ednrb* mutation and to recreate a rat model with severe symptoms, the GK inbred strain was selected, whose haplotype in the responsible region on Chr 2 resembles that of the rat strain in which severe symptoms accompany the *Ednrb^{sl}* mutation. An *Ednrb* mutation was introduced into the GK rat by crossing with F344-*Ednrb^{sl}*. The null mutation of *Ednrb* was found to cause embryonic death in F_2 progeny possessing the GK haplotype in the responsible region on Chr 2. The results of this study are unexpected, and they provide new clues and animal models that

promise to contribute to studies on the genetic regulatory network in the development of

ENS and on embryogenesis.

Table 1. The SNPs in the GK, AGH, F344, and LEH inbred strains

Gene	SNP Location	F344/LEH	AGH/GK
Ptger4	g.73985633, exon 1	T/T	C/T
	g.73986958, promoter	G/G	A/G
	g.73987571, promoter	C/C	T/C
Gdnf	g.76896910, promoter	C/C	T/T
	g.76897291, promoter	C/C	T/T
	g.76901040-76901042, intron 1	TTA/TTA	-/TAA
	g.76901607, intron 1	G/G	A/A
	g.76901863, intron 1	-/G	-/-
	g.76917833-76917835, intron 2	AAG/AAG	-/-
	g.76918613, intron 2	C/C	A/A
	g.76918959, intron 2	G/A	G/G
	g.76919179, intron 2	C/C	T/T
Slc45a2	g.83715441, exon 2	G/G	A/G
	g.83717275, exon 1	C/C	T/C
	g.83717367, exon 1	A/A	T/T
	g.83717975, promoter	A/A	-/-
	g.83718063, promoter	G/G	A/A
	g.83718133, promoter	G/G	A/A

Table 2. The number and ratio of 10-day-old pups possessing the genotype of each microsatellite in the F$_2$(GK × F344) generation

Genotype of Microsatellite / Genotype of *Ednrb* gene	D2Rat201			D2Mgh21			D2Rat19			D2Rat174		
	F/F(%)	F/G(%)	G/G(%)	F/F(%)	F/G(%)	G/G(%)	F/F(%)	F/G(%)	G/G(%)	F/F(%)	F/G(%)	G/G(%)
Ednrb$^{+/+}$	6(31)	8(42)	5(26)	6(31)	8(42)	5(26)	6(31)	8(42)	5(26)	7(37)	7(37)	5(26)
Ednrb$^{sl/+}$	7(29)	12(50)	5(21)	6(25)	13(54)	5(21)	6(25)	14(58)	4(17)	6(25)	14(58)	4(17)
Ednrb$^{sl/sl}$	2(28)	5(71)	0(0)	2(28)	5(71)	0(0)	2(28)	5(71)	0(0)	3(43)	4(57)	0(0)

Table 3. The genome-edited offspring in the F344 and GK strain

Strain	Gene	Number of transferred embryos	Number of litters (%)[a]	Number of offspring (%)[b]	WT offspring	Bi-allelic KO (Phenotype)	Heterozygote/Mosaic (Phenotype)
GK	*Ednrb*	88	1 (25%)	2 (2.3%)	0	0	100% (Early infant death)
	Rosa26	72	2 (66.7%)	2 (2.8%)	0	0	100%
F344	*Ednrb*	23	1 (100%)	4 (17.4%)	0	50% (Mild aganglionosis)	50% (Normal)

[a] Calculate from the total number of female rats used as surrogate.

[b] Calculate from the total number of transferred embryos.
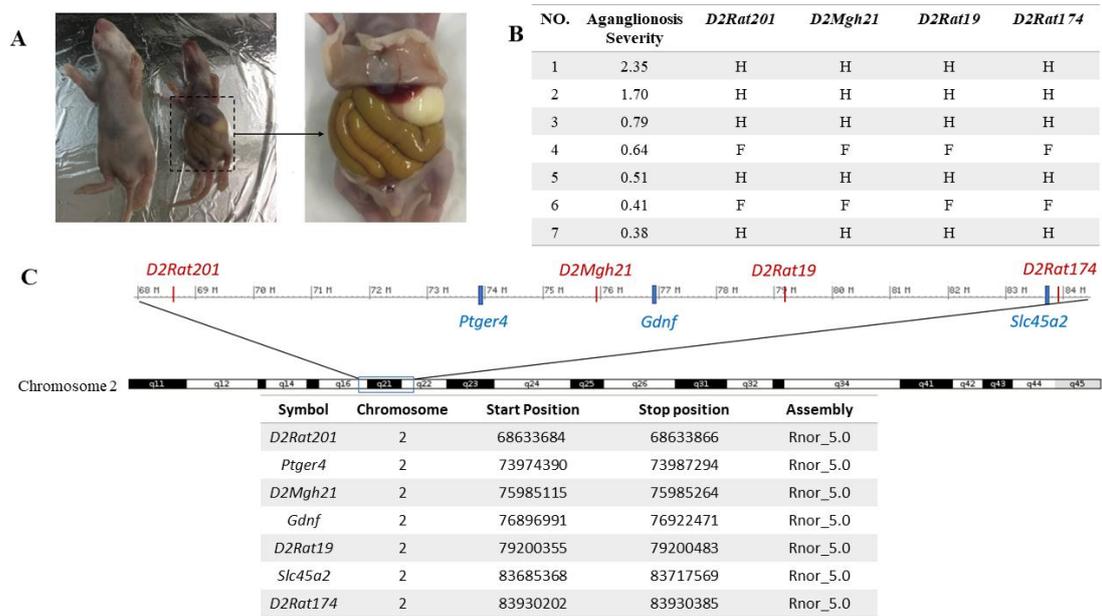
Figure 1. The haplotype and phenotype of F_2(GK × F344)-$Ednrb^{sl/sl}$ progeny.

(A) The 10-day-old offspring of F_2(GK × F344). Right, a pup carrying the *Ednrb*

mutation shows very severe symptom. This pup has an obviously inflated intestine and a

hypoplasia. Left, a healthy littermate. **(B)** The aganglionosis ratio and haplotype for 7

mutant F_2 progeny. The aganglionosis severity was calculated as the aganglionosis ratio

(agangliononic length divided by large intestine length). Four microsatellites located in

the responsible region were selected for the genotyping of the F_2(GK × F344)

generation, and the genotypes of microsatellite loci are listed in the table. F indicates the

homozygous genotype of the F344 strain. H indicates the heterozygous genotype of GK

and F344 rats. No mutant progeny that processed the homozygous genotype of the GK

strain were found. **(C)** A schematic of the identified region on Chr 2. The candidate

genes are marked in blue and the microsatellites are marked in red. The location of each

marker and candidate gene is listed.

Chapter 2

QTL analysis of modifier locus of hooded phenotype in laboratory rats

2.1. Introduction

The rat (*Rattus norvegicus*) has long history of being used in various scientific researches due to advantages of body size and anatomical feature, as well as wide understanding of genetics, diseases, and other benefits for human health. As a visible genetic marker, the coat color of different laboratory rodent has been studied for a long period, and almost 130 genes with 1000 alleles were found related to the variation of pigment type of different mouse strain (54). Hooded is a common pigment pattern in rats that presents coat color in head and various extent of mid-dorsal regions and the diversity of pigmented proportion is observed among different inbred strains, but not individuals (55). Some other modifier alleles related to the specific hooded phenotype are known in previous studies, including Irish (h^i), Notch (h^n), Extreme (h^e) and Restricted (H^{re}) (55-57).

In the previous studies using LEA and IS rats, which are hooded and non-hooded phenotypes, respectively, a hooded locus was mapped to a 460-kb region on Chr 14, in which the *Kit* is the only existing gene (58). *Kit* gene encodes a tyrosine kinase receptor, which plays an important role in regulating the migration, proliferation, differentiations and survival of melanocytes, under the regulation of other factors (59). A further investigation of 172 laboratory rat strains revealed insertion mutations on the first intron

of *Kit* gene in the hooded rat strains (15).

Most of the laboratory rats possess hooded mutations. The F344 rat is one of the most popular inbred strains and shows albino due to the mutation of coat colour gene, tyrosinase (*Tyr*). The F344 rat presents a small pigmentation only in the head region, when wild type of *Tyr* gene is introduced. The LEA rat possesses the same allele of *Kit* gene as F344 rat does, but presents different pattern of hooded phenotype that shows pigmentation in the head and wide region of the dorsal skin. To identify the genetic modifiers that affect the hooded phenotype, QTL analysis was performed using the LEA and F344 rats and a significant QTL was identified in this study.

2.2. Materials and Methods

2.2.1. Animals

Male LEA rats were mated with female F344 rats to produce the F_1 progeny, and the F_2 progeny was generated by mating the F_1 progeny. The animals were maintained in specific pathogen-free conditions with feeding and drinking allowed *ad libitum*. All the F_2 offsprings were euthanized by inhalation of CO_2 at 4 weeks old. All research and experimental protocols were conducted according to the Regulation for the Care and Use of Laboratory Animals of Hokkaido University, and the Animal Use Protocol was approved by the President of Hokkaido University after review by the Animal Care and Use Committee of Hokkaido University (Approval ID: No. 15-0014).

2.2.2. Assessment of pigmented proportion of hooded phenotype

Photographs of both dorsal and ventral sides of each rat were taken with a D3200 camera (Nikon, Tokyo, Japan). The pigmented parts of dorsal and ventral sides were calculated using the histogram function of GIMP 2.8 software (The GIMP Development Team, California, USA) and used as quantitative traits in the QTL analysis.

2.2.3. Microsatellite genotyping

A total number of 78 microsatellite markers covered all chromosomes showing polymorphisms between F344 and LEA rats were selected. Genomic DNAs were extracted from tail tips using the standard methods. PCR was carried out with a touch-down procedure as follows: 1 min at 95 ℃, followed by 10 cycles for 30 sec at 95 ℃, 30 sec at 65-56 ℃, 30 sec at 72 ℃, then 30 cycles for 30 sec at 95 ℃, 30 sec at 55 ℃, 30 sec at 72 ℃, and a final extension at 72 ℃ for 1 min. Totally, 98 F_2(F344 × LEA) animals were used for the genome-wide scan. The amplified products were electrophoresed with 12% polyacrylamide gel and stained with ethidium bromide, then photographed under an ultraviolet lamp.

2.2.4. QTL analysis

QTL analysis was performed with a MapManager QTXb20 software using the genotyping data and pigmented proportion values that collected from F_2(F344 × LEA) offsprings. Permutation tests were done in 1-centi Morgan (cM) steps for 5,000 permutations to identify the likelihood ratio statistic (LRS) values in each chromosome. Further, the permutation tests for two-loci interactions were also conducted by MapManager QTXb20 software using 2,000 permutations in 1-cM steps.

2.2.5. Statistical analysis

A GraphPad Prism software was used for statistical analysis. ANOVA test was used for significance analysis of the pigmented proportion in F344, LEA and F_1 rats, and F_2 progeny with three different genotypes on the identified locus.

2.3. Results

2.3.1. Assessment of pigmented proportion in F_2(F344 × LEA) progeny.

The LEA rat presents a larger pigmented proportion than the typical hooded rats, almost whole dorsal region and part of ventral region are pigmented (Fig. 2A). The photos of dorsal and ventral region of LEA rats were taken and the pigmented proportion of both regions were calculated. As shown in Fig. 3, the coat color covered approximately 93% in the dorsal region and 31% of the ventral region in LEA rats. As a common albino rat strain, color coat is absent in entire body in F344 rats (Fig. 2B), as a consequence of the Tyr^c mutation which hinders the hooded phenotype of F344 rats. Nevertheless, by producing the F_2(F344 × LEA) offsprings, various extents of pigmented proportion were found among the hooded individuals (Fig. 3A and 3B), suggesting that different modifier genes were present between F344 and LEA rats.

2.3.2. QTL analysis for hooded phenotype in F_2(F344 × LEA) rats.

To identify the modifiers that regulate the hooded phenotype of F_2(F344 × LEA) offsprings, QTL analysis was conducted using a MapManager QTXb20 software. Ninety-eight F_2(F344 × LEA) offsprings were genotyped with 78 microsatellites markers (Table 4). The pigmented ratios in dorsal and ventral region were used as

44

quantitative traits for QTL analysis. The LRS was calculated by the software with 5,000 random permutations in 1-cM steps. For the analysis of pigmented proportion in the dorsal region, one highly significant QTL was detected near the *D17Rat2* locus (Fig 4A and 5), which contribute 58% of genetic variance (Table 5). For the analysis of pigmented proportion in ventral region, no significant QTL was identified in all Chrs (Fig 4B). The epistatic interaction analysis between markers were also performed using the MapManager QTXb software, and no significant interaction was identified.

2.3.3. Allelic effects of modifier locus on the pigmented proportion in the dorsal region.

To confirm the effect of identified locus in modifying the pigmented proportion in the dorsal region, the F_2 offsprings were separated into three groups according to their genotypes of the *D17Rat2* locus, which was nearest microsatellite marker to the QTL peak. As shown in Fig. 6, F_2 rats that possessed homozygous LEA allele showed a significantly higher pigmented proportion than others that possessed heterozygous and homozygous F344 alleles. This result indicates that the haplotype of the genomic region near the *D17Rat2* significantly contributes to the pigmented proportion in the dorsal region.

2.4. Discussion

The *Kit* gene encodes a tyrosine kinase receptor, which plays a critical role in regulating the migration, proliferation, differentiation and survival of various cell lineages, including the melanocytic cell lineages (59). The mutations of this gene have been observed in piebaldism patients characterized by congenital patches of skin and hair as a result of absence of melanocytes (60). In mice, mutation of the white spotting (*W*) allele on the *Kit* gene leads to a series of phenotypes, including white coat color, sterility, and anemia (61). The identical phenotypes were also observed in the white spotting rats, which carried a 12-bp deletion on the coding region of *Kit* gene (62, 63). In the previous investigation of 172 laboratory rat strains, insertion of an solitary long terminal repeat (LTR) of rat endogenous retrovirus (ERV) was identified on the first intron of *Kit* gene in Irish hooded strains, and an ERV element was discovered in the same location in the other typical hooded strains and entire albino strains (15). These different insertions may explain the different pigmented ratios between the Irish hooded and other typical hooded; however, the reason for different pigmented ratios of the LEA

rat, which shares the same inserted mutation, is still unknown.

The LEA rat presents a larger pigmented proportion than the typical hooded phenotype but a significantly smaller pigmented proportion than Irish strains, which present pigmentation in whole body, except for the belly region between and behind the front legs (55). In a previous QTL analysis between the LEA rat and the hooded Irish strain, BN, using the pigmented ratio as the quantitative trait, QTLs near the *D14Got14* and *D17Rat2* loci were identified with highly significant statistics and the epistatic interaction between them (64). The *D14Got14* locus is closely located to the position of the hooded locus, inserted mutation in the first intron of *Kit* gene. Therefore, this result is consistent with the different insertions between the Irish and other typical hooded strains (15). In the QTL analysis in this study using the LEA and F344 rats, a QTL near the *D17Rat2* was again identified with the highly significant statistics. As the LEA rats and F344 rats carry the same inserted mutation on the hooded, *Kit*, locus, it is hypothesized that a QTL near the *D17Rat2* locus contains a hooded modifier gene. However, due to the responsible region is too large to confirm the exact modifier genes, it is very difficult to speculate the candidate modifier genes. According to the results of the allelic effect analysis in this study, the LEA allele of the *D17Rat2* locus significantly increased pigmented proportion in the dorsal region of F_2(F344 × LEA) offsprings. The

same result was obtained in the previous QTL analysis; among F_2(BN x LEA) offsprings possessing the homozygous LEA-allele of the *D14Got14* locus, homozygous LEA-allele of the *D17Rat2* locus presented a highest pigmented ratio, followed by heterozygous and homozygous BN-alleles. When the genotype of the *D14Got14* is heterozygous or BN-homozygous, the offsprings displayed similar extent of the pigmented ratio (64). These results suggest that the LEA-haplotype of the genomic region near the *D17Rat2* locus increases pigmented ratio in the hooded phenotype. However, to verify this hypothesis and identify responsible gene/genes on this locus, the generation of congenic strains substituting the genomic region near the *D17Rat2* locus between the LEA and F344 rats is necessary and this trial is under way.

ERV insertions in the first intron of *Kit* gene with antisense orientation were observed in mouse, leading to a small and lower level of transcripts or aberrant splicing (65-67). Considering that the hooded phenotype may be caused by the abnormal expression of the *Kit* gene, it is speculated that a particular haplotype near the *D17Rat2* locus may rescue the dysregulation of this gene. Further studies of the interaction between these loci may provide a better understanding of the gene-regulatory network related to the hooded phenotype. The abnormal expressions of *Kit* gene may cause sterility and anemia as well, and homozygous mutations of this gene usually lead to

severe perinatal lethality (62). The animal models with *Kit* mutation are valuable not only in the studies of the related disorders in human, but also in the application of hematopoietic cells engraftment to the anemia symptom. The appendant phenotype of sterility and lethality may obstruct the preferable application of such animal models. The result in this study that the homozygous LEA-haplotype near the *D17Rat2* locus rescued the phenotype caused by the *Kit* mutation, prompts the possibility that the modifier/modifiers near the *D17Rat2* locus may regulate the *Kit* gene expression and slacking down the other phenotype caused by the mutation of this gene as well. To verify this conjecture, further studies may provide new ideas in improving the performance of *Kit* mutant animal models. In summary, it is suggested that a QTL near the *D17Rat2* locus interacts with the *Kit* gene and plays an important role in regulating expression of the *Kit* gene. The further investigations are necessary to discover modifier(s) and elucidate the genetic mechanisms between these genes.

2.5. Summary

Coat colors of animals, especially laboratory rodents have been studied for more than one hundred years as a visible genetic marker. Hooded phenotype is an interesting pigmented patterns, and mostly observed in laboratory rats, of which pigmentation only present in head and various extend in mid-dorsal region. The hooded mutation was mapped to *Kit* gene in the previous studies, and an insert mutation in the first intron of *Kit* gene was identified; however, the causes of various extents of pigmented proportion in different hooded rat strains are still missing. To reveal modifiers that related the different hooded phenotype, QTL analysis was performed using LEA and F344 rats, both of which carried the same hooded mutation. Even though the F344 present albino coat pattern due to the mutation on *Tyr* gene, the various extents of pigmented proportion were observed in F_2(F344 × LEA) generation, indicating the existence of modifiers. By means of the QTL analysis, a QTL that presented highly significant linkage with the pigmented proportion of dorsal region was identified near the *D17Rat2* on Chr 17. The genotype of *D17Rat2* locus significantly affects the pigmented extent of F_2 progenies. The result of this study confirms the existence of the modifier locus, which interacts with the hooded mutation and affect the hooded phenotype. The modifier locus identified near the *D17Rat2* locus may provide meaningful clues for the

studies of melanocyte development and gene-regulatory network related to the *Kit* gene

in rats.

Table 4. Microsatellite markers used for genotyping F$_2$(F344 × LEA) progeny

Microsatellite Makers	Position (Mbp)	Microsatellite Makers	Position (Mbp)	Microsatellite Makers	Position (Mbp)	Microsatellite Makers	Position (Mbp)
D1Rat250	14.4	D4Rat203	157.8	D10Mgh3	98.9	D15Mgh4	83.9
D1Rat403	47.4	D5Rat121	9.5	D10Rat7	104.3	D16Mgh4	19.4
D1Rat344	122.5	D5Rat190	25.0	D11Rat21	25.0	D16Rat65	61.8
D1Arb29	191.5	D5Mit10	56.9	D11Rat5	57.3	D17Rat2	3.3
D1Rat90	281.8	D5Rat196	103.3	D11Rat43	87.2	D17Rat104	8.7
D2Rat184	39.7	D5Rat33	141.9	D12Rat58	0.5	D17Got20	16.4
D2Arb7	58.3	D6Rat105	19.9	D12Rat76	32.0	D17Rat11	25.5
D2Mit5	66.8	D6Rat136	49.2	D12Rat22	52.0	D17Rat15	32.1
D2Mgh5	106.4	D6Rat3	145.9	D13Rat59	34.6	D17Arb7	64.0
D2Mit8	149.6	D7Mgh11	3.2	D13Mgh4	42.3	D17Rat47	77.9
D2Rat40	169.9	D7Rat112	93.4	D13Mit2	65.0	D18Rat132	25.9
D2Rat52	208.1	D7Rat128	124.2	D13Rat152	91.6	D18Rat92	53.1
D3Mgh7	40.5	D8Rat53	21.8	D14Mit2	19.2	D19Rat82	12.7
D3Mgh6	54.6	D8Rat188	45.3	D14Got35	29.6	D19Rat68	44.6
D3Rat21	115.2	D9Rat46	12.7	D14Got41	34.6	D20Rat37	35.3
D3Mit3	142.0	D9Rat30	21.2	D14Rat15	42.9	D20Mgh1	51.9
D3Rat78	152.5	D9Rat90	81.4	D14Mgh2	78.3	DXRat5	13.9
D4Rat231	89.8	D9Rat4	98.6	D15Rat5	21.0	DXRat50	82.6
D4Rat78	115.8	D9Rat153	107.8	D15Rat6	33.2		
D4Arb28	150.0	D10Mgh6	64.6	D15Rat11	52.8		

Table 5. Characteristics of QTLs detected for extent of pigmented proportion in dorsal or ventral region

| Region	Microsatellite Maker	Position(Mbp)	LRS	%	CI
dorsal	*D7Mgh11*	3.2	9.8	9	57
dorsal	*D7Rat112*	93.4	7.3	7	76
dorsal	*D14Mgh2*	78.3	6.8	7	80
dorsal	*D17Rat2*	4.7	83.4	58	9
dorsal	*D17Rat11*	25.5	12.8	12	44
ventral	*D6Rat3*	145.9	10.1	10	55
ventral	*D14Rat15*	42.9	7.1	7	77
ventral	*D14Mgh2*	78.3	8.1	8	68
ventral	*D15Rat5*	21.0	8.4	8	66
ventral	*D15Rat6*	33.2	9.4	9	59
ventral	*D15Rat11*	52.8	9.3	9	60
ventral	*D16Mgh4*	19.4	8.5	8	65
ventral	*D17Rat2*	4.7	6.7	7	82
ventral	*D17Rat15*	32.6	9.3	9	60
ventral	*D17Arb7*	64.0	12.5	12	45

%: Percentage of total variance attributable to locus.

CI: 95% confidence interval of QTL location as calculated by QTX software.
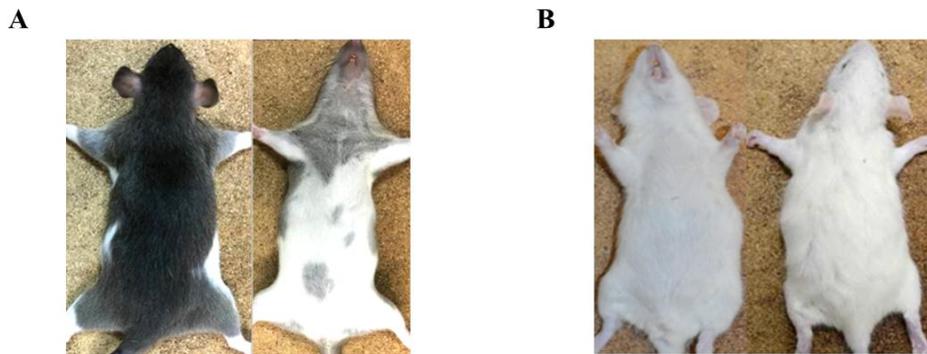
Figure 2. Coat color of LEA and F344 rats

Photos of 4-week-old LEA and F344 rats. **(A)** Dorsal region (left) and ventral region (right) of LEA rat showing hooded phenotype. **(B)** F344 rat showing albino phenotype.
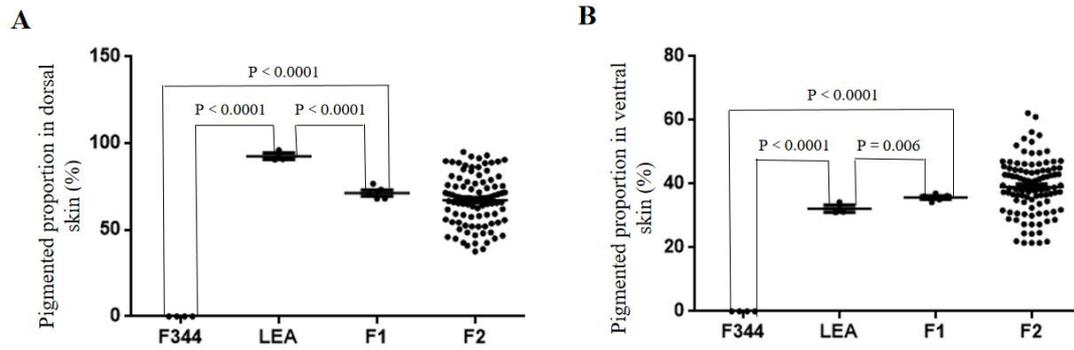
Figure 3. Pigmented proportion of F344, LEA, F$_1$ and F$_2$ animals.

Pigmented proportion in dorsal region **(A)** and ventral region **(B)** of F344, LEA, F$_1$ and

F$_2$ rats. Data are represented as the mean ± SEM. Horizontal lines indicate mean values.
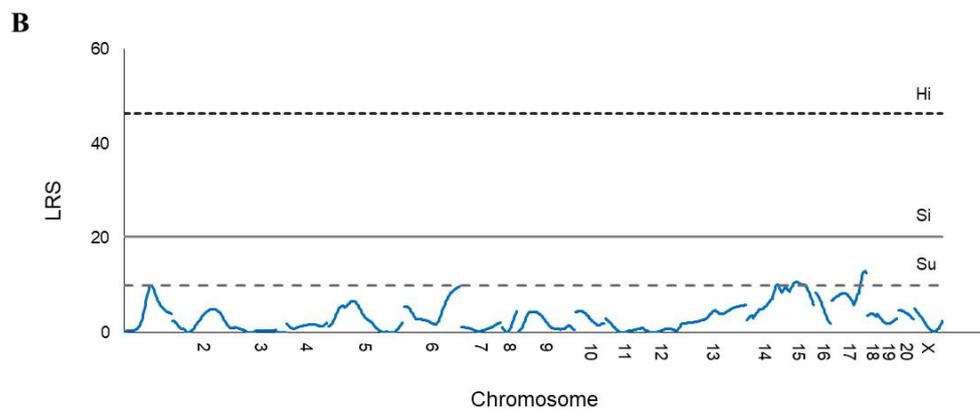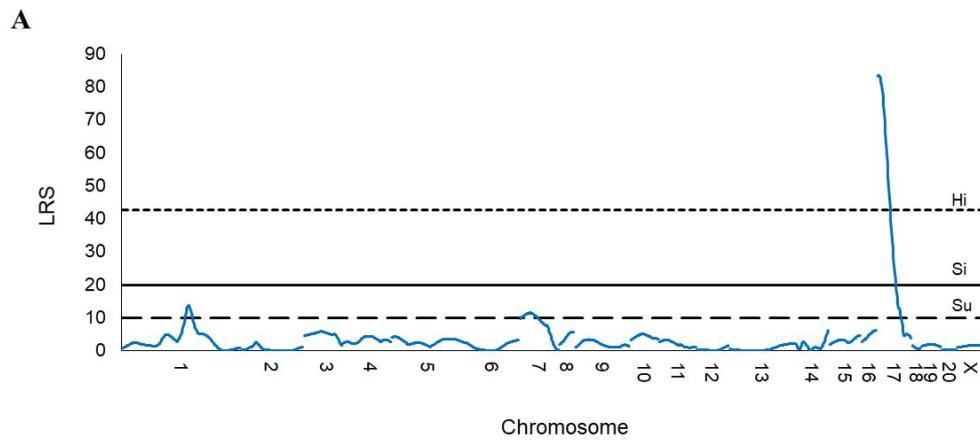
Figure 4. Interval mapping results for dorsal and ventral regions in all Chrs.

A and B show the results of dorsal and ventral regions, respectively. Dense dotted line, full line, and dotted line indicate the highly significant, significant, and suggestive linkage levels, respectively. The vertical axis represents LRS scores.
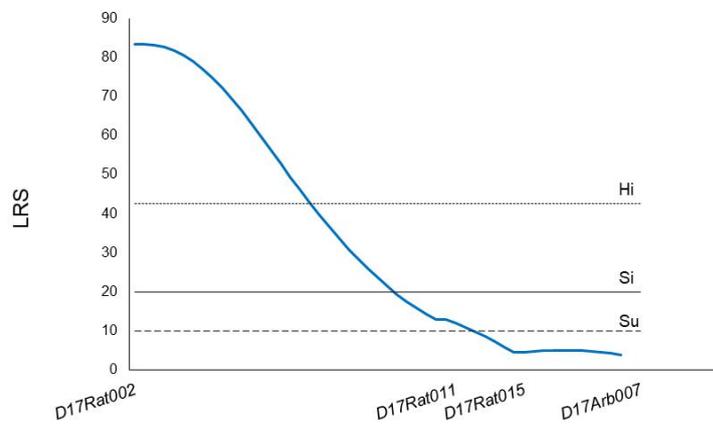
Figure 5. Enlargement of the interval mapping result in Chr 17.

Dense dotted line, full line, and dotted line indicate the highly significant, significant,

and suggestive linkage levels, respectively. The vertical axis represents LRS scores.
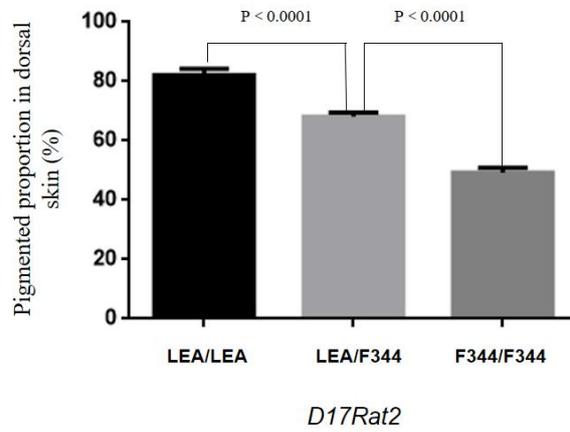
Figure 6. Allelic effects of the *D17Rat2* locus on the pigmented proportion.

Ninety-eight hooded F_2 progeny were separated into three groups according to their genotype of *D17Rat2*, and the pigmented proportion of each group was calculated. Data are represented as the mean ± SEM.

Conclusion

NCCs is one of the most critical cell lineages in the embryogenesis of vertebrates. The discoveries of complex gene-regulatory networks that revolved in the development of various NC-derived cells are never stopped. In this study, genetic analysis of NC-derived two lineages, development of ENS and melanocytes, were conducted using rat models.

In Chapter 1, generation of a new rat strain showing severe phenotype of aganglionosis caused by null mutation of the *Ednrb* gene was tried. To this end, the GK rat was selected, because the GK rat possessed haplotype in the specific region on chromosome 2 similar to that of the AGH rat, which showed the most severe phenotype of aganglionosis caused by null mutation of the *Ednrb* gene by possessing a particular haplotype in the specific region on Chr 2. However, it was found that introduction of null mutation of the *Ednrb* gene caused embryonic lethality in the GK rat. This result proposes the possibility that the *Ednrb* gene interacts with gene(s) located in the critical region on Chr 2 and such interaction plays a critical role in embryogenesis as well as ENS development. The results in this study provide a valuable rat model for further investigation of gene-regulatory networks of the ENS development and embryogenesis.

In Chapter 2, modifier(s) that affect melanocyte development were investigated by

QTL analysis. The LEA and F344 rats were used in this analysis. Although both strains possess the same allele of the *Kit* gene and therefore, showed hooded phenotype, pigmented proportion was different between the two rat strains. The QTL analysis identified a locus near the *D17Rat2* on Chr 17 as responsible for modifying the hooded phenotype. This result suggests that the LEA haplotype of the genomic region including this QTL rescues the dysregulation of melanocytes due to the mutation of *Kit* gene and provides new clues for the studies of melanocyte.

In summary, the results from these two investigations in this study will contribute to better understanding of the roles of NC-derived cells and gene-regulatory networks for the development of NC-derived cells during embryogenesis.

References

1.   Huang X, Saint-Jeannet J-P. Induction of the neural crest and the opportunities of life on the edge. Dev Biol. 2004;275(1):1-11.

2.   Vega-Lopez GA, Cerrizuela S, Aybar MJ. Trunk neural crest cells: formation, migration and beyond. Int J Dev Biol. 2017;61(1-2):5-15.

3.   Simões-Costa M, Bronner ME. Establishing neural crest identity: a gene regulatory recipe. Development. 2015;142(2):242-57.

4.   Theveneau E, Mayor R. Neural crest delamination and migration: from epithelium-to-mesenchyme transition to collective cell migration. Dev Biol. 2012;366(1):34-54.

5.   Dee CT, Szymoniuk CR, Mills PE, Takahashi T. Defective neural crest migration revealed by a Zebrafish model of Alx1-related frontonasal dysplasia. Hum Mol Genet. 2012;22(2):239-51.

6.   McDonald-McGinn DM, Sullivan KE, Marino B, Philip N, Swillen A, Vorstman JA, Zackai EH, Emanuel BS, Vermeesch JR, Morrow BE, Scambler PJ, Bassett AS. 22q11. 2 deletion syndrome. Nat Rev Dis Primers. 2015;1:1−19.

7.   Pingault V, Bondurand N, Kuhlbrodt K, Goerich DE, Préhu M-O, Puliti A,

Herbarth B，Hermans-Borgmeyer I，Legius E，Matthijs G. *SOX10* mutations in patients with Waardenburg-Hirschsprung disease. Nat Genet. 1998;18:171-173.

8.   Simões-Costa M, Bronner ME. Insights into neural crest development and evolution from genomic analysis. Genome Res. 2013;23(7):1069-80.

9.   Sasselli V, Pachnis V, Burns AJ. The enteric nervous system. Dev Biol. 2012;366(1):64-73.

10.   Anderson R, Stewart A, Young H. Phenotypes of neural-crest-derived cells in vagal and sacral pathways. Cell Tissue Res. 2006;323(1):11-25.

11.   Burns AJ, Le Douarin NM. The sacral neural crest contributes neurons and glia to the post-umbilical gut: spatiotemporal analysis of the development of the enteric nervous system. Development. 1998;125(21):4335-47.

12.   Kapur RP. Colonization of the murine hindgut by sacral crest-derived neural precursors: experimental support for an evolutionarily conserved model. Dev Biol. 2000;227(1):146-55.

13.   Mayer TC. The migratory pathway of neural crest cells into the skin of mouse embryos. Dev Biol. 1973;34(1):39-46.

14.   Baxter LL, Hou L, Loftus SK, Pavan WJ. Spotlight on spotted mice: a review of white spotting mouse mutants and associated human pigmentation disorders. Pigment

Cell Res. 2004;17(3):215-24.

15.   Kuramoto T, Nakanishi S, Ochiai M, Nakagama H, Voigt B, Serikawa T. Origins of albino and hooded rats: implications from molecular genetic analysis across modern laboratory rat strains. PloS One. 2012;7(8):e43059.

16.   Badner JA, Sieber WK, Garver KL, Chakravarti A. A genetic study of Hirschsprung disease. Am J Hum Genet. 1990;46(3):568−580.

17.   Amiel J, Sproat-Emison E, Garcia-Barcelo M, Lantieri F, Burzynski G, Borrego S, Pelet A，Arnold S，Miao X，Griseri P. Hirschsprung disease, associated syndromes and genetics: a review. J Med Genet. 2008;45(1):1-14.

18.   Chatterjee S, Kapoor A, Akiyama JA, Auer DR, Lee D, Gabriel S, Berrios C, Pennacchio LA，Chakravarti A. Enhancer variants synergistically drive dysfunction of a gene regulatory network in Hirschsprung disease. Cell. 2016;167(2):355-68. e10.

19.   Brooks A, Oostra B, Hofstra R. Studying the genetics of Hirschsprung's disease: unraveling an oligogenic disorder. Clin Genets. 2005;67(1):6-14.

20.   Heanue TA, Pachnis V. Enteric nervous system development and Hirschsprung's disease: advances in genetic and stem cell studies. Nat Rev Neurosci. 2007;8(6):466−79.

21.   Luo Y, Ceccherini I, Pasini B, Matera I, Bicocchi MP, Barone V, Bocclardi R,

Kääriänen H，Weber D，Devoto M. Close linkage with the RET protooncogene and boundaries of deletion mutations in autosomal dominant Hirschsprung disease. Hum Mol Genet. 1993;2(11):1803-8.

22.　　Kusafuka T, Wang Y, Puri P. Novel mutations of the endothelin-B receptor gene in isolated patients with Hirschsprung's disease. Hum Mol Genet. 1996;5(3):347-9.

23.　　Puffenberger EG, Hosoda K, Washington SS, Nakao K, deWit D, Yanagisawa M, Chakravarti A. A missense mutation of the endothelin-B receptor gene in multigenic Hirschsprung's disease. Cell. 1994;79(7):1257-66.

24.　　Syrris P, Carter ND, Patton MA. Novel nonsense mutation of the endothelin-B receptor gene in a family with Waardenburg-Hirschsprung disease. Am J Med Genet. 1999;87(1):69-71.

25.　　Hofstra RM, Osinga J, Tan-Sindhunata G, Wu Y, Kamsteeg E-J, Stulp RP, van Ravenswaaij-Arts C，Majoor-Krakauer D，Angrist M，Chakravarti A. A homozygous mutation in the endothelin-3 gene associated with a combined Waardenburg type 2 and Hirschsprung phenotype (Shah-Waardenburg syndrome). Nat Genet. 1996;12(4):445－447.

26.　　Angrist M, Bolk S, Halushka M, Lapchak PA, Chakravarti A. Germline mutations in glial cell line-derived neurotrophic factor (*GDNF*) and *RET* in a

Hirschsprung disease patient. Nat Genet. 1996;14(3):341−344.

27.	Salomon R, Attié T, Pelet A, Bidaud C, Eng C, Amiel J, Sarnacki S，Goulet O, Ricour C，Nihoul-Fékété C. Germline mutations of the RET ligand *GDNF* are not sufficient to cause Hirschsprung disease. Nat Genet. 1996;14(3):345−7.

28.	Ruiz-Ferrer M, Torroglosa A, Luzón-Toro B, Fernández RM, Antiñolo G, Mulligan LM, Borrego S. Novel mutations at RET ligand genes preventing receptor activation are associated to Hirschsprung's disease. J Mol Med. 2011;89(5):471-80.

29.	Jiang Q, Ho Y-Y, Hao L, Berrios CN, Chakravarti A. Copy number variants in candidate genes are genetic modifiers of Hirschsprung disease. PLoS One. 2011;6(6):e21219.

30.	Cacheux V, Dastot-Le Moal F, Kääriäinen H, Bondurand N, Rintala R, Boissier B, Wilson M，Mowat D，Goossens M. Loss-of-function mutations in *SIP1* Smad interacting protein 1 result in a syndromic Hirschsprung disease. Hum Mol Genet. 2001;10(14):1503-10.

31.	Szymońska I, Borgenvik TL, Karlsvik TM, Halsen A, Malecki BK, Saetre SE, Jagła M，Kruczek P，Talowska AM，Drabik G. Novel mutation-deletion in the *PHOX2B* gene of the patient diagnosed with Neuroblastoma, Hirschsprung's Disease, and Congenital Central Hypoventilation Syndrome (NB-HSCR-CCHS) Cluster. J Genet

Syndr Gene Ther. 2015;6(3) pmid:26798564.

32.　　Brooks AS, Bertoli-Avella AM, Burzynski GM, Breedveld GJ, Osinga J, Boven LG, Hurst JA，Mancini G MS，Lequin MH，Rene F. Homozygous nonsense mutations in *KIAA1279* are associated with malformations of the central and enteric nervous systems. Am J Hum Genet. 2005;77(1):120-6.

33.　　Amiel J, Attié T, Jan D, Pelet A, Edery P, Bidaud C, Lacombe D，Tam P，Simeoni J，Flori E. Heterozygous Endothelin Receptor B (*EDNRB* Mutations in Isolated Hirschsprung Disease. Hum Mol Genet. 1996;5(3):355-7.

34.　　Attié T, Till M, Pelet A, Amiel J, Edery P, Boutrand L, Munnich A，Lyonnet S. Mutation of the endothelin-receptor B gene in Waardenburg-Hirschsprung disease. Hum Mol Genet. 1995;4(12):2407-9.

35.　　Gariepy CE, Cass DT, Yanagisawa M. Null mutation of endothelin receptor type B gene in spotting lethal rats causes aganglionic megacolon and white coat color. Proc Natl Acad Sci U S A. 1996;93(2):867-72.

36.　　Dang R, Torigoe D, Suzuki S, Kikkawa Y, Moritoh K, Sasaki N, Agui T. Genetic background strongly modifies the severity of symptoms of Hirschsprung disease, but not hearing loss in rats carrying *Ednrb^{sl}* mutations. PLoS One. 2011;6(9):e24086.

37.   Dang R, Torigoe D, Sasaki N, Agui T. QTL analysis identifies a modifier locus

of aganglionosis in the rat model of Hirschsprung disease carrying *Ednrb^sl* mutations.

PloS One. 2011;6(11):e27902.

38.   Huang J, Dang R, Torigoe D, Lei C, Lan X, Chen H, Sasaki N, Wang J, Agui

T. Identification of genetic loci affecting the severity of symptoms of Hirschsprung

disease in rats carrying *Ednrb^sl* mutations by quantitative trait locus analysis. PloS One.

2015;10(3):e0122068.

39.   Cantrell VA, Owens SE, Chandler RL, Airey DC, Bradley KM, Smith JR,

Southard-Smith EM. Interactions between *Sox10* and *EdnrB* modulate penetrance and

severity of aganglionosis in the *Sox10* ^Dom mouse model of Hirschsprung disease. Hum

Mol Genet. 2004;13(19):2289-301.

40.   Kaneko T, Sakuma T, Yamamoto T, Mashimo T. Simple knockout by

electroporation of engineered endonucleases into intact rat embryos. Sci Rep.

2014;4:6382.

41.   McCallion AS, Stames E, Conlon RA, Chakravarti A. Phenotype variation in

two-locus mouse models of Hirschsprung disease: tissue-specific interaction between

Ret and *Ednrb*. Proc Natl Acad Sci U S A. 2003;100(4):1826-31.

42.   Welsh IC, O'Brien TP. Loss of Late Primitive Streak Mesoderm and

Interruption of Left–Right Morphogenesis in the *Ednrb^{s-1Acrg}* Mutant Mouse. Dev Biol. 2000;225(1):151-68.

43.   Semenova E, Wang X, Jablonski MM, Levorse J, Tilghman SM. An engineered 800 kilobase deletion of *Uchl3* and *Lmo7* on mouse chromosome 14 causes defects in viability, postnatal growth and degeneration of muscle and retina. Hum Mol Genet. 2003;12(11):1301-12.

44.   Galli J, Li L-S, Glaser A, Östenson C-G, Jiao H, Fakhrai-Rad H, Jacob HJ, Lander ES, Luthman H. Genetic analysis of non-insulin dependent diabetes mellitus in the GK rat. Nat Genet. 1996;12(1):31−37.

45.   Momose K, Nunomiya S, Nakata M, Yada T, Kikuchi M, Yashiro T. Immunohistochemical and electron-microscopic observation of β-cells in pancreatic islets of spontaneously diabetic Goto–Kakizaki rats. Med Mol Morphol. 2006;39(3):146-53.

46.   Gauguier D, Froguel P, Parent V, Bernard C, Bihoreau M-T, Portha B, James MR, Penicaud L, Lathrop M, Ktorza A. Chromosomal mapping of genetic loci associated with non-insulin dependent diabetes in the GK rat. Nat Genet. 1996;12(1):38−43.

47.   Granhall C, Park H-B, Fakhrai-Rad H, Luthman H. High-resolution

quantitative trait locus analysis reveals multiple diabetes susceptibility loci mapped to intervals< 800 kb in the species-conserved Niddm1i of the GK rat. Genetics. 2006;174(3):1565-72.

48.   McKeown SJ, Mohsenipour M, Bergner AJ, Young HM, Stamp LA. Exposure to GDNF enhances the ability of enteric neural progenitors to generate an enteric nervous system. Stem Cell Reports. 2017;8(2):476-88.

49.   Shen L, Pichel JG, Mayeli T, Sariola H, Lu B, Westphal H. *Gdnf* haploinsufficiency causes Hirschsprung-like intestinal obstruction and early-onset lethality in mice. Am J Hum Genet. 2002;70(2):435-47.

50.   Huang J, Dang R, Torigoe D, Li A, Lei C, Sasaki N, Wang J, Agui T. Genetic variation in the GDNF promoter affects its expression and modifies the severity of Hirschsprung's disease (HSCR) in rats carrying *Ednrb*[sl] mutations. Gene. 2016;575(1):144-8.

51.   M.W. Moore, R.D. Klein, I. Fariñas, H. Sauer, M. Armanini, H. Phillips, L.F. Reichardt, A.M. Ryan, K. Carver-Moore, A. Rosenthal. Renal and neuronal abnormalities in mice lacking GDNF. Nature. 1996;382(6586):76-79.

52.   Pichel J G, Shen L, Sheng H Z, Granholm A-C, Drago J, Grinberg A, Lee E J, Huang S P, Saarma M, Hoffer B J, Sariola H, Westphal H. Defects in enteric innervation

and kidney development in mice lacking GDNF. Nature. 1996;382(6586):73–76.

53.   Sánchez MP, Silos-Santiago I, Frisén J, He B, Lira SA, Barbacid M. Renal agenesis and the absence of enteric neurons in mice lacking GDNF. Nature. 1996;382(6586):70−73.

54.   Steingrímsson E, Copeland NG, Jenkins NA. Mouse coat color mutations: from fancy mice to functional genomics. Dev Dyn. 2006;235(9):2401-11.

55.   Castle W. Variation in the hooded pattern of rats, and a new allele of hooded. Genetics. 1951;36(3):254−266.

56.   GUMBRECK LG, STANLEY AJ, MACY RM, PEEPLES EE. Pleiotropic expression of the restricted coat-color gene in the Norway rat. J Hered. 1971;62(6):357-8.

57.   Robinson R. An extreme allele of hooded spotting in the Norway rat. Genetica. 1989;79(2):139-41.

58.   Torigoe D, Ichii O, Dang R, Ohnaka T, Okano S, Sasaki N, Kon Y, Agui T. High-resolution linkage mapping of the rat hooded locus. J Vet Med Sci. 2011;73(5):707-10.

59.   Grichnik JM. Kit and melanocyte migration. Journal of Investigative Dermatology. 2006;126(5):945-7.

60. Giebel LB, Spritz RA. Mutation of the *KIT* (mast/stem cell growth factor receptor) protooncogene in human piebaldism. Proc Natl Acad Sci U S A. 1991;88(19):8696-9.

61. Geissler EN, Ryan MA, Housman DE. The dominant-white spotting (W) locus of the mouse encodes the c-kit proto-oncogene. Cell. 1988;55(1):185-92.

62. Niwa Y, Kasugai T, Ohno K, Morimoto M, Yamazaki M, Dohmae K, Nishimune Y，Kondo K，Kitamura, Y. Anemia and mast cell depletion in mutant rats that are homozygous at" white spotting (Ws)" locus. Blood. 1991;78(8):1936-41.

63. Tsujimura T, Hirota S, Nomura S, Niwa Y, Yamazaki M, Tono T, Morii E，Kim HM，Kondo K，Nishimune Y. Characterization of Ws mutant allele of rats: a 12-base deletion in tyrosine kinase domain of *c-kit* gene. Blood. 1991;78(8):1942-6.

64. Torigoe D, Asano A, Yamauchi H, Dang R, Sasaki N, Agui T. Genetic analysis of modifiers for the hooded phenotype in the rat. Jpn J Vet Res. 2010;57(4):175-84.

65. Bowes C, Li T, Frankel WN, Danciger M, Coffin JM, Applebury ML, Farber, DB. Localization of a retroviral element within the rd gene coding for the beta subunit of cGMP phosphodiesterase. Proc Natl Acad Sci U S A. 1993;90(7):2955-9.

66. Bultman SJ, Klebig ML, Michaud EJ, Sweet HO, Davisson MT, Woychik RP. Molecular analysis of reverse mutations from nonagouti (a) to black-and-tan (a (t)) and

white-bellied agouti (Aw) reveals alternative forms of agouti transcripts. Genes Dev. 1994;8(4):481-90.

67.   Hofmann M, Harris M, Juriloff D, Boehm T. Spontaneous Mutations in SELH/Bc Mice Due to Insertions of Early Transposons: Molecular Characterization of Null Alleles at thenudeandalbinoLoci. Genomics. 1998;52(1):107-9.

Acknowledgements

Summary in Japanese

　　神経堤細胞は脊椎動物の胚発生において最も重要な細胞系列の一つである。様々な神経堤細胞由来細胞の発達に作用する複雑な遺伝子制御ネットワークの発見がなされている。本研究では、ラットを用い、神経堤細胞由来の二つの細胞系列、腸管神経システムとメラノサイトの発達について遺伝学的解析を行った。

　　第 1 章では、エンドセリンレセプタータイプ B (*Ednrb*)遺伝子のヌル変異によって引き起こされる重症の腸管神経節欠損症を示す新規のラットモデルの樹立を試みた。この目的のために GK ラットが選択された。その理由は、GK ラットは *Ednrb* 遺伝子のヌル変異を持った時に重症の腸管神経節欠損症を示す原因とされる第 2 染色体の特定部位において、同じく *Ednrb* 遺伝子のヌル変異を持った時に最も重症の腸管神経節欠損症を呈する AGH ラットと同様のハプロタイプを持っているためである。しかしながら GK ラットに *Ednrb* 遺伝子のヌル変異を導入すると胎生致死を呈することがわかった。この結果は *Ednrb* 遺伝子が第 2 染色体の特定部位に存在する遺伝子と相互作用し、この相互作用が腸管神経システムの発達だけでなく胚の発生にも重要な役割を演じていることを示唆している。この研究結果は、腸管神経システムの発達と胚発生における遺伝

子制御ネットワークの研究を更に深める有用なラットモデルとなるであろう。

　　第 2 章では、メラノサイトの発達に影響を与える修飾因子について QTL 解析を用いて研究を行なった。この解析においては LEA ラットと F344 ラットが用いられた。両系統とも *Kit* 遺伝子に同じ変異を有し、その結果被毛色は頭巾斑を呈するが、両系統間で異なる有色被毛率を示す。QTL 解析の結果、第 17 染色体の *D17Rat2* マイクロサテライト近傍に頭巾斑を修飾する責任遺伝子座（QTL）が存在することが同定された。この結果は、この QTL を含むゲノム領域が LEA ハプロタイプの時には *Kit* 遺伝子の変異によるメラノサイトの発達不全がレスキューされることを示唆しており、メラノサイトの発達を研究する上で新しい手がかりを提供している。

　　これら二つの研究結果は、胚発生時の神経堤細胞由来細胞の役割とその発達における遺伝子制御ネットワークの解明に貢献することが期待される。